

# Relativistic light-on-heavy nuclear collisions and the implied rapidity asymmetry

Adeola Adeluyi,<sup>1</sup> Gergely G. Barnaföldi,<sup>1,2</sup> George Fai,<sup>1</sup> and Péter Lévai<sup>2</sup>

<sup>1</sup>*Center for Nuclear Research, Department of Physics  
Kent State University, Kent, OH 44242, USA*

<sup>2</sup>*MTA KFKI RMKI Research Institute for Particle and Nuclear Physics  
P.O. Box 49, Budapest 1525, Hungary*

(Dated: October 30, 2018)

We calculate pseudorapidity ( $\eta$ ) asymmetry in  $pA$  and  $dA$  collisions in a pQCD-improved parton model. With the calculations tuned to describe existing spectra from  $pp$  collisions and asymmetric systems at midrapidity and large rapidities at FNAL and RHIC energies, we investigate the roles of nuclear shadowing and multiple scattering on the observed asymmetry. Using this framework, we make predictions for pseudorapidity asymmetries at high  $p_T$  and large  $\eta$  in a wide range of energies up to LHC.

PACS numbers: 24.85.+p, 25.30.Dh, 25.75.-q

## I. INTRODUCTION

Collisions of asymmetric nuclear systems, like proton-nucleus or deuteron-nucleus collisions, attract significant experimental and theoretical attention at present. At the Relativistic Heavy Ion Collider (RHIC), Run 8 included deuteron-gold collisions at 200 AGeV with a luminosity increase of about an order of magnitude compared to the deuteron-gold run of 2003. One of the physics goals was to provide a high-statistics “cold” nuclear matter data set to establish a definitive baseline for “hot” nuclear matter, created in gold-gold collisions. The benchmark role of the “the deuteron-gold control experiment” for e.g. energy-loss studies has often been emphasized [1, 2]. Proton-nucleus and deuteron-nucleus reactions were also used to study the Cronin-effect [3, 4].

Light-on-heavy nucleus-nucleus collisions offer unique information about the underlying dynamics, not available in symmetric proton-proton or nucleus-nucleus collision systems. The light-on-heavy asymmetry manifests itself in an asymmetric (pesudo-)rapidity distribution of charged particles with respect to zero rapidity (or pseudorapidity) as measured by BRAHMS [5] and PHOBOS [6]. The asymmetry of the yields can be quantified by introducing the ratio of pseudorapidity densities at a given negative pseudorapidity relative to that at the positive pseudorapidity of the same magnitude. This backward/forward ratio (forward being the original direction of motion of the light partner) is referred to as pseudorapidity asymmetry. The STAR Collaboration published pseudorapidity asymmetries in 200 AGeV  $dAu$  collisions for several identified hadron species and total charged hadrons in the pseudorapidity intervals  $|\eta| \leq 0.5$  and  $0.5 \leq |\eta| \leq 1.0$  [7]. Asymmetries with the backward/forward ratio above unity for transverse momenta up to  $\approx 5$  GeV/ $c$  are observed for charged pion, proton+anti-proton, and total charged hadron production in both rapidity regions. Because of the importance of asymmetric collisions, we anticipate that proton-lead or deuteron-lead data will be collected at the Large Hadron Collider (LHC).

The theoretical relevance of asymmetric collision systems (in particular colliding the lightest nuclei like protons or deuterons on a heavy partner) in testing parameterizations for nuclear shadowing and models for initial multiple scattering was recognized prior to the availability of 200 AGeV RHIC deuteron-gold data [8, 9, 10]. One can take advantage of the fact that positive (forward) rapidities correspond to large parton momentum fractions from the light partner and small momentum fractions from the heavy nucleus (and vice versa for negative rapidities), and that there are more collisions suffered traversing the heavy partner. Wang made predictions for pseudorapidity asymmetries on this basis [9]. A subsequent calculation focused on the lowest transverse momenta where pQCD may be applicable [11]. More recently, two versions of a pQCD-based model with nuclear modifications were used to address deuteron-gold collisions and results were compared to available data [12, 13]. The related subject of forward-backward rapidity correlations in asymmetric systems is treated in [14] using a derivative of string percolation models, and in [15] under the framework of color glass condensate.

In the present study we investigate the roles of nuclear shadowing and multiple scattering in the generation of rapidity asymmetry in the backward/forward yields at intermediate and high transverse-momenta. Here we use the HIJING shadowing parameterization [16] and the recently released Eskola–Paukkunen–Salgado (EPS08) nuclear parton distribution functions (nPDFs) [17]. While the former has been applied widely, the latter was not available at the time of the earlier studies mentioned above. We calculate the pseudorapidity asymmetry in three representative asymmetric light-on-heavy systems:  $pBe$  at 30.7 GeV (Fermilab),  $dAu$  at 200 AGeV (RHIC), and  $dPb$  at 8.8 ATeV (LHC). We concentrate on neutral pion production and compare results to experimental data from the E706 experiment [18], PHENIX [19], and STAR [7].

The paper is organized as follows: in Sec. II we review the basic formalism of the pQCD-improved parton model with intrinsic transverse momentum and multiple scat-

tering as applied to proton-nucleus ( $pA$ ) and deuteron-nucleus ( $dA$ ) collisions. This section also includes the definition of the pseudorapidity asymmetry and a discussion of the roles of nuclear shadowing and multiple scattering in asymmetric collisions. We present the results of our calculation in Sec. III and conclude in Sec. IV.

## II. CALCULATIONAL FRAMEWORK

### A. Description of the model

The invariant cross section for the production of final hadron  $h$  from the collision of nucleus  $A$  and nucleus  $B$  ( $A+B \rightarrow h+X$ ), can be written, in collinearly factorized pQCD, as

$$E_h \frac{d^3 \sigma_{AB}^h}{d^3 p} = \sum_{abcd} \int d^2 b \, d^2 r \, t_A(b) t_B(|\vec{b} - \vec{r}|) dx_a dx_b \int dz_c f_{a/A}(x_a, Q^2) f_{b/B}(x_b, Q^2) \frac{d\sigma(ab \rightarrow cd)}{d\hat{t}} \frac{D_{h/c}(z_c, Q_f^2)}{\pi z_c^2} \hat{s} \delta(\hat{s} + \hat{t} + \hat{u}), \quad (1)$$

where  $x_a$  and  $x_b$  are parton momentum fractions in  $A$  and  $B$ , respectively, and  $z_c$  is the fraction of the parton momentum carried by the final-state hadron  $h$ . The factorization and fragmentation scales are  $Q$  and  $Q_f$ , respectively. As usual,  $\hat{s}$ ,  $\hat{t}$ , and  $\hat{u}$  refer to the partonic Mandelstam variables, the massless parton approximation is used, and

$$t_A(\vec{s}) = \int dz \rho_A(\vec{s}, z) \quad (2)$$

is the Glauber thickness function of nucleus  $A$ , with the nuclear density distribution,  $\rho_A(\vec{s}, z)$  subject to the normalization condition

$$\int d^2 s \, dz \rho_A(\vec{s}, z) = A. \quad (3)$$

The quantity  $d\sigma(ab \rightarrow cd)/d\hat{t}$  in eq. (1) represents the perturbatively calculable partonic cross section, and  $D_{h/c}(z_c, Q_f^2)$  stands for the fragmentation function of parton  $c$  to produce hadron  $h$ , evaluated at momentum fraction  $z_c$  and fragmentation scale  $Q_f$ .

The collinear parton distribution functions (PDFs) can be generalized to include a transverse momentum degree of freedom,  $\vec{k}_T$ , as required by the uncertainty principle. This can be formally implemented in terms of unintegrated PDFs [20, 21]. To avoid some of the complications associated with using unintegrated PDFs, it is expedient to parameterize phenomenologically the  $\vec{k}_T$  dependence of the parton distributions. In this light a phenomenological model for proton-proton ( $pp$ ), proton-nucleus ( $pA$ ), and nucleus-nucleus ( $AB$ ) collisions incorporating parton transverse momentum in the collinear pQCD formalism was developed in Ref. [22]. In order to make the present

study reasonably self-contained, we include details relevant to the present treatment.

In this model, the invariant cross section can be written as

$$E_h \frac{d^3 \sigma_{AB}^h}{d^3 p} = \sum_{abcd} \int d^2 b \, d^2 r \, t_A(b) t_B(|\vec{b} - \vec{r}|) dx_a dx_b \int d\vec{k}_{Ta} \, d\vec{k}_{Tb} \, dz_c f_{a/A}(x_a, \vec{k}_{Ta}, Q^2) f_{b/B}(x_b, \vec{k}_{Tb}, Q^2) \frac{d\sigma(ab \rightarrow cd)}{d\hat{t}} \frac{D_{h/c}(z_c, Q_f^2)}{\pi z_c^2} \hat{s} \delta(\hat{s} + \hat{t} + \hat{u}), \quad (4)$$

where the  $k_T$ -broadened parton distribution in the nucleon is written, in a simple product approximation, as

$$f_{a/N}(x, \vec{k}_T, Q^2) \longrightarrow g(\vec{k}_T) \cdot f_{a/N}(x, Q^2), \quad (5)$$

with  $f_{a/N}(x, Q^2)$  denoting the standard collinear PDF in the nucleon. The transverse momentum distribution is taken to be a Gaussian,

$$g(\vec{k}_T) = \frac{\exp(-k_T^2 / \langle k_T^2 \rangle_{pp})}{\pi \langle k_T^2 \rangle_{pp}}, \quad (6)$$

where  $\langle k_T^2 \rangle_{pp}$  is the two-dimensional width of the transverse-momentum distribution in the proton. Based on the then-available pion and unidentified hadron production data, an estimate for the model width of the transverse-momentum distribution of partons in the proton ( $\langle k_T^2 \rangle_{pp}$ ) was presented in Ref. [22]. A recent summary of the energy dependence of the model parameter  $\langle k_T^2 \rangle$ , related to the average transverse momentum of the created pair by

$$\langle k_T^2 \rangle_{pp} = \frac{\langle p_T \rangle_{pair}^2}{\pi}, \quad (7)$$

can be found in Ref. [23]. The value of  $\langle k_T^2 \rangle_{pp}$  increases logarithmically with  $\sqrt{s}$ , and the data are well described by the function

$$\langle p_T \rangle_{pair} = (1.74 \pm 0.12) \cdot \log_{10}(\sqrt{s}) + (1.23 \pm 0.2). \quad (8)$$

Using eq. (8) one can estimate  $\langle k_T^2 \rangle$  at required cms energies. It should be noted that eq. (8) is a fit to the data at lower energies. Since no data exists at LHC energies, we extrapolate  $\langle k_T^2 \rangle$ . We observe that: (a) Since the dependence is logarithmic, the energy step we make from RHIC to LHC is comparable to the one from SPS to RHIC. We thus do not a priori expect a radical change in the trend. (b) The  $k_T$  effects have been shown to be appreciable at low  $p_T$ , and since our predictions at LHC cover a wide  $p_T$  range up to hundreds of GeV/c in  $p_T$ , potential uncertainties arising from the extrapolation of Eq. 8 will affect a small fraction of this range at the low  $p_T$  end. (c) The present study, at LHC energies, is exploratory. Results of pp collisions at the LHC will be helpful in determining the magnitude of the presently uncertain  $\langle k_T^2 \rangle_{pp}$ .

It is easy to appreciate the physical necessity of the presence of a transverse-momentum degree of freedom

in proton-proton and, therefore, nuclear collisions. However, the handling of the effect of the nuclear environment on transverse momenta is one of the specific features of the given description. Most shadowing parameterizations include at least some of the effects of multiple scattering in the nuclear medium, while the HIJING parameterization (as we discuss further in Sec. II C) needs to be augmented with modeling nuclear multiscattering. For this purpose, in  $pA$  collisions we use a broadening of the width of the transverse momentum distribution (6) according to

$$\langle k_T^2 \rangle_{pA} = \langle k_T^2 \rangle_{pp} + C h_{pA}(b), \quad (9)$$

where  $\langle k_T^2 \rangle_{pp}$  is the width already present in proton-proton collisions,  $h_{pA}(b)$  is the number of effective nucleon-nucleon ( $NN$ ) collisions as a function of nucleon impact parameter  $b$ , and  $C$  is the average increase in width per  $NN$  collision. In nucleus-nucleus ( $AB$ ) collisions, the  $p_T$  distributions of both nuclei are subject to the broadening represented by eq. (9).

The function  $h_{pA}(b)$  can be written in terms of the number of collisions suffered by the incoming proton in the target nucleus,  $\nu_A(b) = \sigma_{NN} t_A(b)$ , where  $\sigma_{NN}$  is the inelastic nucleon-nucleon cross sections. It was found in Ref. [22] that only a limited number of collisions is effective in broadening the transverse momentum distribution. This model scenario was referred to as “saturation”, and an optimal description was found with the effective number of nucleon-nucleon collisions maximized at 4, and the average width increase per  $NN$  collision,  $C$ , set to  $0.35 \text{ GeV}^2/c^2$ . We do not change the values of these parameters in the present study. The resulting transverse momentum broadening may appear too large relative to what is observed in Drell-Yan data at FNAL. However, we focus on meson production in the present application, where the PHENIX experiment extracts intrinsic transverse momenta in  $pp$  collisions at RHIC energies that are similar in magnitude to the ones discussed here [24]. Further details about this aspect of the model can be found in Ref. [22].

The intrinsic transverse momentum  $k_T$  is treated phenomenologically in Ref. [22] and in the present study. While next-to-leading-order (NLO) calculations provide a more accurate description of the parton-level cross section, they continue to rely on the factorization theorem and represent the non-perturbative information in terms of PDFs and fragmentation functions. Since these functions are fitted to the same data as in LO, the expected change is a shift in responsibility between the perturbative and non-perturbative sectors in describing the data used to define the non-perturbative ingredients. In applications to a larger set of data this will not eliminate the need for the phenomenological use of a transverse momentum distribution, in particular considering the fact that even NLO may be far from a full perturbative expansion. In addition, above we argue for inclusion of a transverse momentum degree of freedom on fundamental physical grounds as basic as the uncertainty principle.

The simple Gaussian representation of this physics provides a phenomenologically useful additional parameter (the width). This holds true both at the LO and NLO levels. Going to NLO may change the range of transverse momenta where intrinsic  $k_T$  is important (see e.g. Refs. [25, 26, 27]). No attempt is made in the present work to discuss the  $x$ , flavor (quarks and gluons), and rapidity dependence of  $k_T$ . We have limited ourselves here to a simple effective description. This seems adequate for now, since  $k_T$  effects are appreciable only at relatively low  $p_T$ , and a major focus of this work is asymmetry at high  $p_T$  (except at very forward rapidities where  $p_T$ -s are low due to phase space constraints). The intrinsic transverse momentum,  $\langle k_T^2 \rangle_{pp}$ , enhances hadron production yields at low  $p_T$  in both negative and positive pseudorapidity regions, thus tending to cancel out in the asymmetry ratio. Multiscattering, on the other hand, does impact appreciably on the asymmetry even at low  $p_T$ . Overall, calculations within this framework have proven their value in the interpretation of hadron-production data [22, 28]. (For a comparison of the leading-order  $k_T$ -factorized approach and next-to-leading order collinear approach see Ref. [29].)

The collinear nPDFs  $f_{a/A}(x, Q^2)$  are expressible as convolutions of nucleonic parton distribution functions (PDFs)  $f_{a/N}(x, Q^2)$  and a shadowing function  $\mathcal{S}_{a/A}(x, Q^2)$  which encodes the nuclear modifications of parton distributions. We use the MRST2001 PDFs [30] for the nucleon parton distributions, and for the shadowing function we employ both the EPS08 shadowing routine [17] and HIJING [16]. (Other nPDFs, like FGS [31], HKN [32], and the earlier EKS [33], are used elsewhere to calculate pseudorapidity asymmetries [12].) For the final hadron fragmentation we utilize the fragmentation functions in the AKK set [34]. The factorization scale is tied to the parton transverse momentum via  $Q = (2/3)p_T/z_c$ , while the fragmentation scale varies with the transverse momentum of the outgoing hadron, according to  $Q_f = (2/3)p_T$ , following the best-fit results obtained in Ref. [35]. This scale fixing is not modified from earlier applications, and is used consistently throughout the present calculations. To protect against divergences in the partonic cross sections, a cutoff regulator mass is necessary. We have tested the sensitivity of our calculations at different cms energies by varying the regulator mass between  $0.5 - 2.0 \text{ GeV}$ . For  $p_T > 1.5 \text{ GeV}/c$  our results show little sensitivity to variation of regulator mass. We present results for  $p_T > 2.25 \text{ GeV}/c$  here, and thus regulator mass effects are expected to be minimal. We obtain the density distribution of the deuteron from the Hulthen wave function [36] (as in Ref. [37]), while a Woods-Saxon density distribution is used for gold and lead with parameters from Ref. [38].

## B. Forward and backward nuclear modifications

The nuclear modification factor is designed to compare, as a ratio, spectra of particles produced in nuclear collisions to a hypothetical scenario in which the nuclear collision is assumed to be a superposition of the appropriate number of nucleon-nucleon collisions. The ratio can be defined as a function of  $p_T$  for any produced hadron species  $h$  at any pseudorapidity  $\eta$ :

$$R_{AB}^h(p_T, \eta) = \frac{1}{\langle N_{bin} \rangle} \cdot \frac{E_h d^3 \sigma_{AB}^h / d^3 p |_{\eta}}{E_h d^3 \sigma_{pp}^h / d^3 p |_{\eta}}, \quad (10)$$

where  $\langle N_{bin} \rangle$  is the average number of binary collisions in the various impact-parameter bins. Nuclear effects manifest themselves in  $R_{AB}^h(p_T, \eta)$  values greater or smaller than unity, representing enhancement or suppression, respectively, relative to the  $NN$  reference.

In asymmetric collisions, hadron production at forward rapidities may be different from what is obtained at backward rapidities. It is thus of interest to study ratios of particle yields between a given pseudorapidity value and its negative in these collisions. The pseudorapidity asymmetry  $Y_{Asym}(p_T)$  is defined for a hadron species  $h$  as

$$Y_{Asym}^h(p_T) = E_h \frac{d^3 \sigma_{AB}^h}{d^3 p} \Big|_{-\eta} / E_h \frac{d^3 \sigma_{AB}^h}{d^3 p} \Big|_{\eta}. \quad (11)$$

Let us consider the (double) ratio of the forward and backward nuclear modification factors in  $dAu$  collisions for species  $h$ :

$$R_{\eta}^h(p_T) = \frac{R_{dAu}^h(p_T, -\eta)}{R_{dAu}^h(p_T, \eta)} = \frac{E_h d^3 \sigma_{dAu}^h / d^3 p |_{-\eta}}{E_h d^3 \sigma_{pp}^h / d^3 p |_{-\eta}} / \frac{E_h d^3 \sigma_{dAu}^h / d^3 p |_{\eta}}{E_h d^3 \sigma_{pp}^h / d^3 p |_{\eta}}. \quad (12)$$

As discussed in Ref. [13], since the  $pp$  rapidity distribution is symmetric around  $y = 0$ , if the same backward and forward (pseudo)rapidity ranges are taken in both directions (i.e.  $|\eta_{min}| \leq |\eta| \leq |\eta_{max}|$ ), then the  $pp$  yields cancel in eq. (12) and one obtains that the ratio defined in (12) is identical to the pseudorapidity asymmetry (11):

$$Y_{Asym}^h(p_T) = R_{\eta}^h(p_T) = \frac{R_{dAu}^h(p_T, -\eta)}{R_{dAu}^h(p_T, \eta)}. \quad (13)$$

Eq. (13) is useful from the experimental point of view to handle the systematic errors of data and extract the proper pseudorapidity asymmetry. It also provides a connection between measured rapidity asymmetry and the nuclear modification factors.

## C. Nuclear shadowing and multiple scattering

We expect that particle production in  $pA$  ( $dA$ ) collisions will have different yields in the forward and backward directions. This is because the respective partons

have different momentum fractions (shadowing differences) and because the forward-going parton has to traverse a large amount of matter. We found in our earlier studies that the HIJING shadowing parameterization is particularly useful for the study of multiple scattering, as it requires an explicit treatment of  $k_T$  broadening (see eq. (9)) for a successful description of data [22]. In this Section we therefore study the interplay of shadowing and multiple scattering in more detail using the HIJING parameterization.

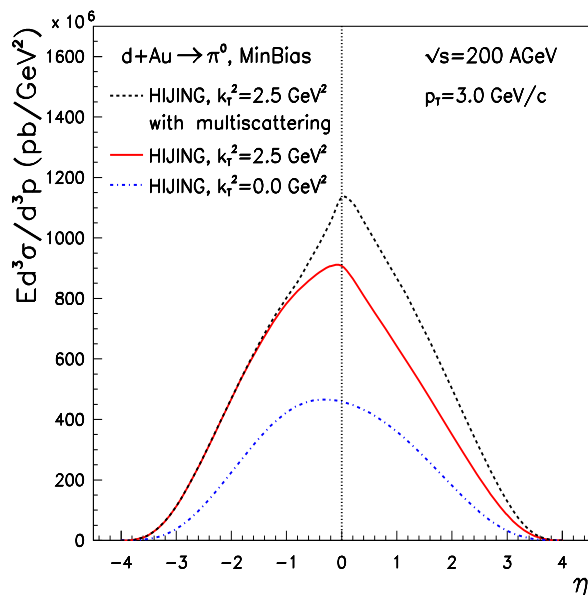


FIG. 1: (Color Online) Illustration of calculated yields at  $p_T = 3.0$  GeV/c in minimum bias neutral pion production from  $dAu$  collisions at 200 AGeV. The solid line represents HIJING shadowing with intrinsic  $k_T$  in the proton, the dashed line is HIJING with intrinsic  $k_T$  and multiple scattering, while the dot-dashed curve is obtained by turning off any transverse momentum.

In Fig. 1 we display the neutral pion yield as a function of pseudo-rapidity in  $dAu$  collisions at a fixed  $p_T$ , namely at 3.0 GeV/c. This illustrates how the nuclear effects we examine modify the asymmetry of the yields. The figure shows the calculated distribution using the HIJING shadowing parameterization without any intrinsic  $k_T$  (dot-dashed curve), using HIJING shadowing and including the intrinsic  $k_T$  in the nucleon (solid), and HIJING shadowing with intrinsic  $k_T$  and multiple scattering (dashed). The parameters of eq. (9) are unchanged from our previous studies at midrapidity [28, 35], and we have chosen a transverse momentum value comparable to  $\langle k_T \rangle_{pp}$ , where the various effects are clearly displayed.

We checked that when shadowing and all nuclear effects are turned off, the distribution is symmetric around midrapidity, as expected. With shadowing only, we find an asymmetry in the distribution: the yield at a fixed



negative pseudorapidity, say  $\eta = -2$  (*Au* side or “backward”) is higher than at the corresponding positive pseudorapidity ( $\eta = 2$ , *d* side, or “forward”). Thus the pseudorapidity asymmetry,  $Y_{Asym}$ , is greater than unity in this case. The inclusion of the intrinsic transverse momentum in the proton significantly increases the yields on both the *Au* side and the *d* side at this transverse momentum, as it makes larger  $p_T$ -s accessible. We tested that adding intrinsic transverse momentum in the proton in the absence of shadowing does not destroy the forward/backward symmetry. When intrinsic  $k_T$  in the proton is added to the calculation using shadowing, but without the multiple scattering contribution, the sense of the asymmetry given by shadowing (backward/forward  $\geq 1$ ) is preserved. However, when multiple scattering is included, the yield shows a stronger increase in the forward direction. This is understandable in the present picture, since forward-going products originate in the partons of the deuteron, and have to traverse a large amount of nuclear matter resulting in strong multiple scattering, while the backward products suffer no or little multiple scattering. This has the effect of reversing the asymmetry: the yield on the *d*-side is now greater than that on the *Au*-side. The calculated pseudorapidity asymmetry,  $Y_{Asym}$ , turns out to be less than unity in this case. An alternative way to summarize the situation is to say that shadowing suppresses the yield more on the *d* side (forward) relative to a symmetric collision, while the multiple scattering contribution is understandably large in the forward direction.

We have carried out similar studies at higher  $p_T$  values. When the intrinsic transverse momenta are small relative to the  $p_T$  of the final hadron,  $k_T$  effects become naturally smaller. Shadowing effects also become smaller as the antishadowing region of the HIJING parameterization is approached. Thus, at  $p_T \gtrsim 15$  GeV/*c* the influence of multiple scattering and intrinsic  $k_T$  become negligible. These phenomena are most important at intermediate  $p_T$  values,  $2$  GeV/*c*  $\lesssim p_T \lesssim 8$  GeV/*c* at RHIC. It is interesting to note that a similar transverse-momentum region is sensitive to nuclear effects at lower (e.g. CERN SPS) energies, due to the  $\sim \log(\sqrt{s})$  scaling of the Cronin peak [23, 39, 40].

### III. RESULTS

To judge the success of the model in reproducing spectra, here we first present calculated spectra for neutral pion production at midrapidity and non-zero rapidities. This will help select the model choices providing the best agreement with the experimental information. The selected model variants are then used to calculate pseudorapidity asymmetries.

#### A. Midrapidity spectra

Figure 2 displays midrapidity RHIC  $\pi^0$  spectra from *dAu* collisions at  $|\eta| < 0.35$ , and for reference, the spectra from *pp* collisions at the same energy ( $\sqrt{s} = 200$  AGeV). The results are compared to data from the PHENIX collaboration [19]. In the top left panel we show calculated *dAu* spectra using EPS08 nPDFs with and without intrinsic  $k_T$  in the proton, but without any multiple scattering contribution. The top right depicts the *dAu* spectra using HIJING plus  $k_T$  with and without multiple scattering. The bottom panels contain data/theory (i.e. data/model) ratios. As can be seen clearly in the bottom left *dAu* data/theory panel, including intrinsic  $k_T$  in the proton increases the calculated yield mostly at low  $p_T$ . We consider the EPS08 description with intrinsic  $k_T$  in the proton satisfactory in the  $4$  GeV/*c*  $\lesssim p_T \lesssim 10$  GeV/*c* interval. Comparing the two bottom data/theory panels it is easy to see that the HIJING parameterization gives a very similar accuracy for *dAu* when multiple scattering is included. This is also very close to the data/theory for *pp* collisions given by HIJING.

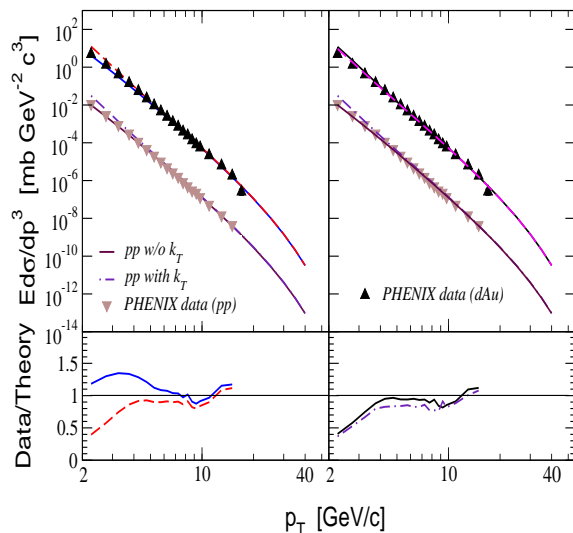


FIG. 2: (Color Online) Top: spectra for *dAu*  $\pi^0$  production at  $|\eta| < 0.35$ . The left panel shows EPS08 with (dashed) and without (solid) intrinsic  $k_T$ . The right panel is HIJING plus  $k_T$  with (solid) and without (dashed) multiple scattering. Filled triangles denote the PHENIX data [19]. The *pp* spectra from the same experiment and calculated with (dashed) and without (solid) intrinsic  $k_T$  are also included. Bottom: corresponding data/theory ratios for (left) *dAu* with and without  $k_T$  and (right) *pp* with  $k_T$  and HIJING plus  $k_T$  with multiple scattering.

Fig. 3 shows the spectra for neutral pion production from *pBe* collisions at  $|\eta| < 0.2$ . The top left panel

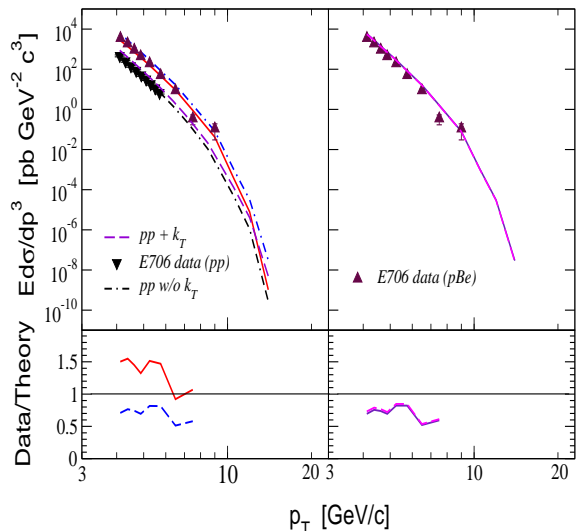


FIG. 3: (Color Online) Spectra for  $p + Be \rightarrow \pi^0 + X$  at  $|\eta| < 0.2$ . The left panel depicts EPS08 calculations with (dashed) and without (solid) intrinsic  $k_T$ . The right panel is HIJING plus  $k_T$  with (solid) and without (dashed) multiple scattering. Filled triangles denote the E706 data [18]. Data and calculations for proton-proton (pp) collisions are at 530 GeV/c.

shows the spectra using EPS08 nPDFs with and without intrinsic  $k_T$ . The top right depicts the spectra using HIJING plus  $k_T$  with and without multiple scattering. The agreement with the E706 data from Fermilab is quite good as can be seen from the lower panels which display the data per theory ratio. The HIJING parameterization with and without multiple scattering gives almost identical data/theory ratios, i.e. multiple scattering has only a small effect on spectra from  $pBe$  collisions. This is reasonable in view of the fact that in the light  $Be$  nucleus there are few scattering centers. The effect of intrinsic  $k_T$  is to increase the calculated yield, leading to data/theory ratios less than unity for all relevant  $p_T$ .

We conclude from Figs 2 and 3 that it is necessary to include the intrinsic transverse momentum of partons in the proton in our model to obtain a satisfactory description of available data. The EPS08 and HIJING parameterizations differ to the extent that while HIJING calls for the inclusion of the broadening of the intrinsic transverse momentum distribution via multiple scattering, EPS08 appears to incorporate this physics in their nPDFs. We thus concentrate on three model variants (EPS08 with proton intrinsic  $k_T$  and HIJING with intrinsic  $k_T$  and with/without multiscattering) in the remainder of this study.

## B. Spectra at non-zero rapidities

We now consider spectra at non-zero pseudorapidities. We display results from EPS08 with proton intrinsic  $k_T$  and HIJING with intrinsic  $k_T$  and multiscattering. Fig. 4 shows the spectra and corresponding data/theory ratio for  $p + Be \rightarrow \pi^0 + X$  at  $-0.7 < \eta < -0.2$  (“backward”, left panel) and  $0.2 < \eta < 0.7$  (“forward”, right panel) using EPS08 nPDFs with  $k_T$  and HIJING plus  $k_T$  with multiscattering. The two sets (EPS08 and HIJING) give very similar data/theory ratios for both pseudorapidity intervals. There is reasonable agreement with the E706 data [18] as is apparent from the quality of the data/theory ratios.

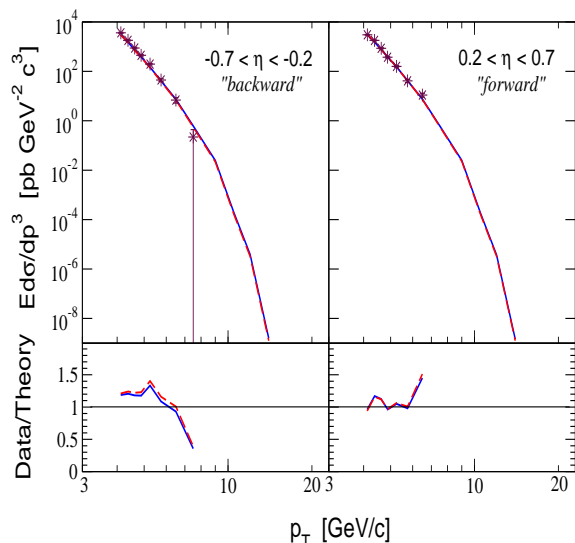


FIG. 4: (Color Online) Spectra for  $p + Be \rightarrow \pi^0 + X$  at  $-0.7 < \eta < -0.2$  (left panel) and  $0.2 < \eta < 0.7$  (right panel). The solid lines represent the EPS08 nPDFs with intrinsic  $k_T$ , while the dashed line is obtained from HIJING plus  $k_T$  with the inclusion of multiscattering. Stars denote the E706 data [18].

The  $dAu$  spectra are displayed in Fig. 5 for both EPS08 and HIJING at  $-1.0 < \eta < -0.5$  (left panel) and  $0.5 < \eta < 1.0$  (right panel). Note that the experimental data from the STAR collaboration [7] are not separated into negative and positive pseudorapidities, but rather averaged over both intervals. Therefore, the data points in Fig. 5 only serve to guide the eye; the relevance of the Figure is to highlight the difference between the EPS08 and HIJING results visible in the bottom panels. It can be seen that the EPS08 results do not differ much in the forward and backward directions, while HIJING gives significantly larger data/theory ratios forward. Thus, EPS08 and HIJING differ appreciably at forward pseudorapidities,  $0.5 < \eta < 1.0$ . This is not unexpected, because multiple scattering influences the  $d$ -

side (forward) more than the  $Au$ -side (backward). To be able to draw stronger conclusions, separated forward and backward data will be necessary, hopefully forthcoming from the high-statistics Run 8.

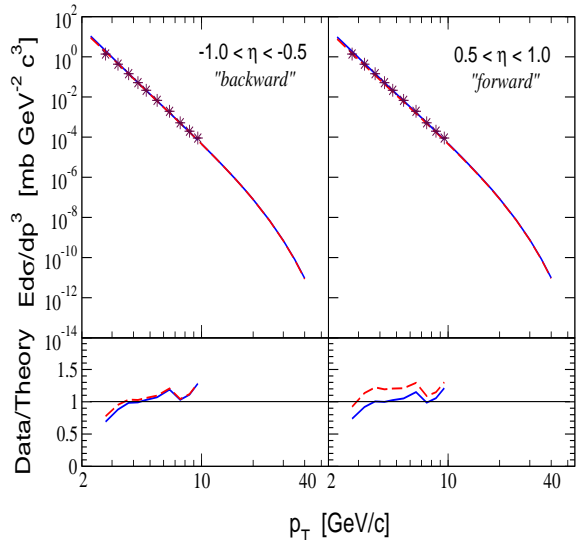


FIG. 5: (Color Online) Spectra for  $d + Au \rightarrow \pi^0 + X$  at  $-1.0 < \eta < -0.5$  (left panel) and  $0.5 < \eta < 1.0$  (right panel). The solid line represents the EPS08 with intrinsic  $k_T$ , while the dashed line is obtained from HIJING plus  $k_T$  with the inclusion of multiscattering. Stars denote STAR data averaged over  $0.5 < |\eta| < 1.0$

### C. Pseudorapidity asymmetry

#### 1. Asymmetry in $pBe$ collisions at 30.7 GeV

The pseudorapidity asymmetry for the rapidity interval  $0.2 < |\eta| < 0.7$  is shown in the upper panel of Fig. 6 compared with the E706 data [18]. The solid line represents EPS08 with proton intrinsic  $k_T$ , the dot-dashed line displays HIJING with intrinsic  $k_T$ , and the dashed is HIJING plus intrinsic  $k_T$  and multiple scattering. Both EPS08 with  $k_T$  and HIJING without multiple scattering give very small asymmetries and the data are also consistent with  $Y_{Asym} = 1$  for low  $p_T$ . The HIJING parameterization with multiple scattering yields somewhat lower values at all transverse momenta. This is in line with the effect of multiple scattering moderately increasing the yield on the  $p$ -side relative to that of the  $Be$ -side. In view of the rather large error bars, all three sets are in reasonable agreement with the data. The lower panel is our prediction for the interval  $1.0 < |\eta| < 1.5$ . Here, the calculated effects are larger, but have a similar structure

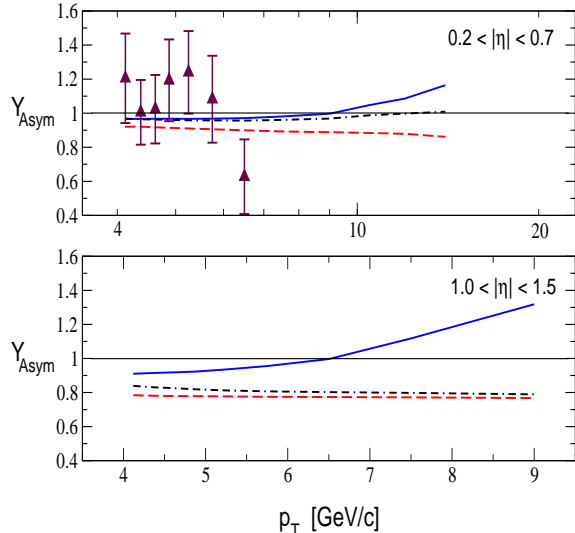


FIG. 6: (Color Online) Pseudorapidity asymmetry,  $Y_{Asym}$  for  $p + Be \rightarrow \pi^0 + X$  at  $0.2 < |\eta| < 0.7$  (top) and  $1.0 < |\eta| < 1.5$  (bottom). The solid line represents the EPS08 nPDFs, while the dashed line is obtained from HIJING with the inclusion of multiscattering. The dot-dashed line corresponds to HIJING without multiscattering, and filled triangles denote the E706 data [18].

to what is seen at lower  $\eta$ . This trend is similar to what will be seen at other energies.

#### 2. Asymmetry in $dAu$ collisions at 200 AGeV

Figure 7 shows the pseudorapidity asymmetry for  $\pi^0$  production from  $dAu$  collisions at RHIC, for different pseudorapidity intervals. The two uppermost panels are our results for the asymmetry at  $|\eta| < 0.5$  and  $0.5 < |\eta| < 1.0$  compared with the STAR data [7]. For  $p_T > 4.0$  GeV/c, the agreement with data is quite good for all three sets. At lower  $p_T$ , multiple scattering increases the calculated yield mostly in the forward direction as discussed in Sec. II C, leading to asymmetries below unity. At very high  $p_T$  we observe a divergence in the model predictions. The lower four panels are our predictions for the asymmetry as pseudorapidity increases. The first three of these correspond to the BRAHMS pseudorapidity intervals [41]. The general trend is that the asymmetry becomes larger as  $\eta$  increases. This mainly arises from the strong shadowing in the larger nucleus at lower  $x$  values. Also, since increasing  $\eta$  leads to decreasing accessible  $p_T$  due to phase space constraints, the effects of multiple scattering become more pronounced. In fact, for the largest  $\eta$  considered,  $3.7 < |\eta| < 4.3$ , there is a marked difference between HIJING with and without

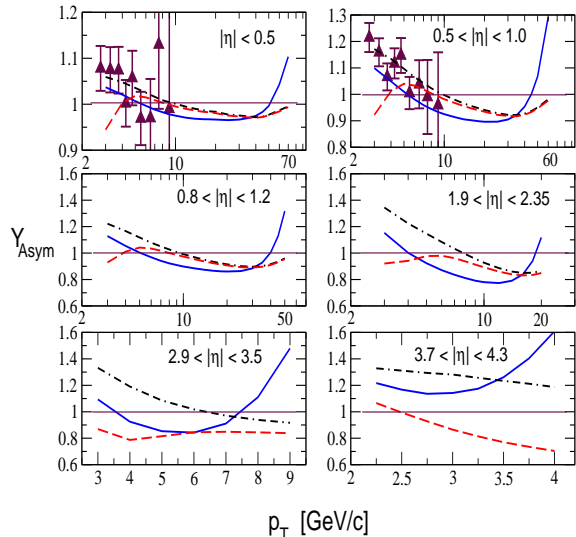


FIG. 7: (Color Online) Pseudorapidity asymmetry,  $Y_{Asym}$  for  $d + Au \rightarrow \pi^0 + X$  at different pseudorapidity intervals. The solid line represents the EPS08 nPDFs, while the dashed line is obtained using HIJING shadowing with the inclusion of multiscattering. The dot-dashed line corresponds to HIJING without multiscattering, and filled triangles denote the STAR data [7].

multiple scattering for all  $p_T$  considered.

It is pertinent at this point to make some remarks about pseudorapidity asymmetry in the BRAHMS pseudorapidity intervals. The BRAHMS Collaboration [41] has observed a progressive suppression of both minimum bias nuclear modification  $R_{dAu}$  and central-to-peripheral ratios,  $R_{CP}$ , with increasing  $\eta$ . The present study is limited to minimum bias pseudorapidity asymmetry, and both shadowing parameterizations (EPS08 and HIJING) adequately describe the existing experimental data at very forward rapidities. The EPS08 parameterization incorporates RHIC data at large rapidities, i.e. at low  $x$ , and thus reproduces the data. Therefore, at least in the minimum bias case, shadowing seems sufficient for a good description of the suppression observed at low  $x$ . The situation is different for the geometry-dependent  $R_{CP}$ , where ( $b$ -independent) shadowing plus conjectured impact parameter dependencies [12, 42] are clearly inadequate in describing the observed suppression.

### 3. Asymmetry in $dPb$ collisions at 8.8 ATeV

Let us now turn to our predictions for the pseudorapidity asymmetry in a potential future  $dPb$  collision at LHC energy of 8.8 ATeV. The calculated results are displayed in Fig. 8, where the upper panel is for the interval

$|\eta| < 0.9$  and the lower panel is for  $2.4 < |\eta| < 4.0$ . These intervals correspond to acceptance in the central detector and in the muon arm, respectively, of the ALICE experiment [44]. All three sets predict minimal asymmetry of the order of a few percent for the interval  $|\eta| < 0.9$ . As we

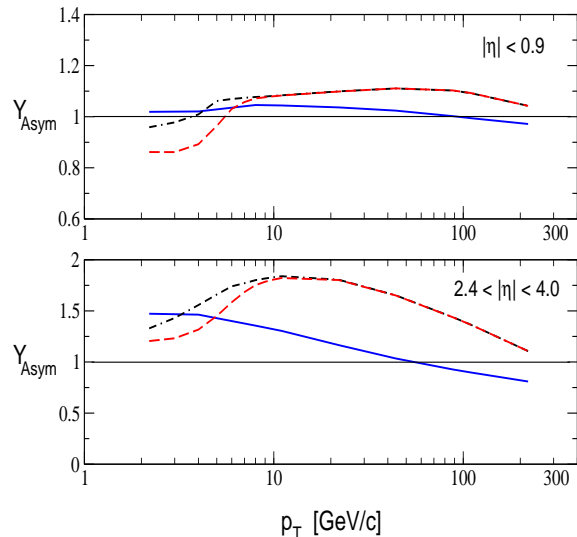


FIG. 8: (Color Online) Predicted pseudorapidity asymmetry,  $Y_{Asym}$  for  $d + Pb \rightarrow \pi^0 + X$  at  $\sqrt{s} = 8.8$  ATeV for  $|\eta| < 0.9$  and  $2.4 < |\eta| < 4.0$ . The solid line represents the EPS08 nPDFs, while the dashed line is obtained from HIJING with the inclusion of multiscattering. The dot-dashed line corresponds to HIJING without multiscattering.

move to higher  $\eta$ , the predicted asymmetry becomes more significant. As can be seen in the lower panel of Fig. 8, both EPS08 and HIJING predict substantial asymmetry up to  $\sim 10$  GeV/c, and both variants of HIJING asymmetries remaining significant up to  $\sim 100$  GeV/c, in contrast to EPS08.

At the present level, neither model variant gives agreement with all aspects of the data: in an earlier calculation we have found that shadowing parameterizations which do not need to be augmented by a multiple scattering prescription [31, 32, 33] have difficulty describing central-to-peripheral ratios at forward rapidity [12]. We have checked that this also holds for the EPS08 nPDFs. On the other hand, the HIJING parameterization with multiscattering yields pseudorapidity asymmetries below unity at low transverse momenta. This deficiency may be cured by allowing an  $\eta$ -dependent multiscattering [45].

## IV. CONCLUSION

Here we give a concise summary of the results of our calculations. We have demonstrated the usefulness of



asymmetric (light-on-heavy) nuclear collisions at relativistic energies. As illustrated in Sec. II C, the physical differences between forward- and backward-going produced particles arise from the different ranges of  $x$  sampled (different shadowing) and different amount of multiple scattering. This leads to observable pseudorapidity asymmetries at some collision energies and transverse momenta. We have considered the effects of nuclear shadowing and multiple scattering on pseudorapidity asymmetry for three asymmetric systems:  $pBe$ ,  $dAu$ , and  $dPb$  in a wide energy range.

To calibrate and fine-tune our model we first examined spectra of produced neutral pions. We found that there are two avenues in the model for the reasonable description of these data: (i) HIJING shadowing, intrinsic  $k_T$ , plus multiscattering, or (ii) some other nPDFs (we use EPS08 here) and intrinsic  $k_T$  (but no additional multiscattering). We then calculated pseudorapidity asymmetries with these prescriptions. Overall, the calculated asymmetries are in reasonable agreement with available experimental data. Intrinsic transverse momentum in the nucleon is seen to be important at low  $p_T$ . Multiple scattering increases the yield in the “forward” or positive pseudorapidity region, thus leading to a tendency for asymmetries less than unity at low  $p_T$  in the scheme ex-

plicitely relying on multiple scattering, at variance with the data. An LHC measurement at a high pseudorapidity and high  $p_T$  (where  $k_T$  effects no longer make a difference) may be able to distinguish between strong shadowing (as in the HIJING prescription) and an nPDF with a relatively weaker gluon suppression (like e.g. EPS08).

A major constraint in assessing pseudorapidity asymmetries is the limited availability of data for direct comparison with theoretical calculations. More data in asymmetric light-on-heavy collisions separated with respect to positive and negative pseudorapidities are needed to judge calculated pseudorapidity asymmetries. At RHIC, it is expected that the high-statistic  $dAu$  Run 8 is going to provide such a large data set.

## V. ACKNOWLEDGMENTS

This work was supported in part by Hungarian OTKA PD73596, T047050, NK62044, and IN71374, by the U.S. Department of Energy under grant U.S. DOE DE-FG02-86ER40251, and jointly by the U.S. and Hungary under MTA-NSF-OTKA OISE-0435701.

- 
- [1] M. Gyulassy, *J. Phys. G* **30**, S911 (2004).  
[2] T. K. Hemmick, *J. Phys. G* **30**, S659 (2004).  
[3] Cronin J W *et al* (CP Collaboration) 1975 *Phys. Rev.* **D11** 3105  
[4] Antreasyan D *et al* (CP Collaboration) 1979 *Phys. Rev.* **D19** 764  
[5] I. Arsene *et al.* [BRAHMS Collaboration], *Phys. Rev. Lett.* **94**, 032301 (2005).  
[6] B. B. Back *et al.* [PHOBOS Collaboration], *Phys. Rev. C* **72**, 031901 (2005).  
[7] B. I. Abelev *et al.* [STAR Collaboration], *Phys. Rev. C* **76**, 054903 (2007); J. Adams *et al.* [STAR Collaboration], *Phys. Rev. C* **70**, 064907 (2004).  
[8] I. Vitev, *Phys. Lett. B* **562**, 36 (2003).  
[9] X. N. Wang, *Phys. Lett. B* **565**, 116 (2003).  
[10] G. G. Barnafoldi, G. Papp, P. Levai and G. Fai, *J. Phys. G* **30**, S1125 (2004)  
[11] G. G. Barnafoldi, P. Levai, G. Papp and G. Fai, *Nucl. Phys. A* **749**, 291 (2005).  
[12] A. Adelyi and G. Fai, *Phys. Rev. C* **76**, 054904 (2007).  
[13] G. G. Barnafoldi, A. Adelyi, G. Fai, P. Levai and G. Papp, arXiv:0807.3384 [hep-ph].  
[14] P. Brogueira, J. Dias de Deus and J. G. Milhano, *Phys. Rev. C* **76**, 064901 (2007)  
[15] N. Armesto, L. McLerran and C. Pajares, *Nucl. Phys. A* **781**, 201 (2007)  
[16] S. J. Li and X. N. Wang, *Phys. Lett. B* **527**, 85 (2002).  
[17] K. J. Eskola, H. Paukkunen and C. A. Salgado, *JHEP* **0807**, 102 (2008)  
[18] L. Apanasevich *et al.* [Fermilab E706 Collaboration], *Phys. Rev. D* **68**, 052001 (2003).  
[19] S.S. Adler *et al.* [PHENIX Collaboration], *Phys. Rev. Lett.* **91**, 072303 (2003); *Phys. Rev.* **C74**, 024904 (2006).  
[20] J. C. Collins, T. C. Rogers and A. M. Stasto, *Phys. Rev. D* **77**, 085009 (2008).  
[21] M. Czech and A. Szczurek, *J. Phys. G* **32**, 1253 (2006).  
[22] Y. Zhang, G. I. Fai, G. Papp, G. G. Barnafoldi and P. Levai, *Phys. Rev. C* **65**, 034903 (2002).  
[23] G. G. Barnafoldi, P. Levai, G. Fai, G. Papp and B. A. Cole, *Int. J. Mod. Phys. E* **16**, 1923 (2007)  
[24] S. S. Adler *et al.* [PHENIX Collaboration], *Phys. Rev. D* **74**, 072002 (2006)  
[25] A. D. Martin, W. J. Stirling and R. G. Roberts, *Phys. Lett. B* **354**, 155 (1995)  
[26] J. Huston, E. Kovacs, S. Kuhlmann, H. L. Lai, J. F. Owens and W. K. Tung, *Phys. Rev. D* **51**, 6139 (1995)  
[27] D. de Florian, W. Vogelsang and F. Wagner, *Phys. Rev. D* **76**, 094021 (2007)  
[28] P. Levai, G. Papp, G. G. Barnafoldi and G. I. Fai, *Eur. Phys. J. ST* **155**, 89 (2008).  
[29] A. Szczurek, A. Rybarska and G. Slipek, *Phys. Rev. D* **76**, 034001 (2007).  
[30] A. D. Martin, R. G. Roberts, W. J. Stirling and R. S. Thorne, *Eur. Phys. J. C* **23**, 73 (2002).  
[31] L. Frankfurt, V. Guzey and M. Strikman, *Phys. Rev. D* **71**, 054001 (2005).  
[32] M. Hirai, S. Kumano and T. H. Nagai, *Phys. Rev. C* **70**, 044905 (2004); *Nucl. Phys. Proc. Suppl.* **139**, 21 (2005).  
[33] K. J. Eskola, V. J. Kolhinen and C. A. Salgado, *Eur. Phys. J. C* **9**, 61 (1999).  
[34] S. Albino, B. A. Kniehl and G. Kramer, *Nucl. Phys. B* **725**, 181 (2005).  
[35] P. Levai, G. G. Barnafoldi, G. Fai and G. Papp, *Nucl.*

- Phys. A **783**, 101 (2007).
- [36] L. Hulthen and M. Sugawara, "Handbuch der Physik", vol. 39 (1957).
- [37] D. Kharzeev, E. Levin and M. Nardi, Nucl. Phys. A **730**, 448 (2004) [Erratum-ibid. A **743**, 329 (2004)].
- [38] C. W. De Jager, H. De Vries and C. De Vries, Atom. Data Nucl. Data Tabl. **14**, 479 (1974).
- [39] L. Apanasevich *et al.*, Phys. Rev. D **59**, 074007 (1999); L. Apanasevich *et al.* [Fermilab E706 Collaboration], Phys. Rev. Lett. **81**, 2642 (1998).
- [40] M. Zielinski, arXiv:hep-ph/9811278.
- [41] I. Arsene *et al.* [BRAHMS Collaboration], Phys. Rev. Lett. **93**, 242303 (2004).
- [42] R. Vogt, Phys. Rev. C **70**, 064902 (2004).
- [43] H. Yang [BRAHMS Collaboration], J. Phys. G **34**, S619 (2007)
- [44] B. Alessandro *et al.* [ALICE Collaboration], J. Phys. G **32**, 1295 (2006).
- [45] G. G. Barnafoldi and G. Fai, work in progress